

Hydrogenation Properties of the TiB_x Structures

R. Žitko¹, H. J. P. Van Midden¹, E. Zupanič¹, A. Prodan^{1*}, S. S. Makridis^{2,5}, D. Niarchos³ and A. K. Stubos⁴

¹Jožef Stefan Institute, Jamova 39, SI-1000 Ljubljana, Slovenia

²Department of Mechanical Eng., University of Western Macedonia, Kozani, GR-50100, Greece

³Inst. of Material Science, NCSR Demokritos, Athens, GR-15310 Greece

⁴Inst. of Nuclear Technol. and Rad. Protection, NCSR Demokritos, Athens, GR-15310 Greece

⁵Hystore Technologies Ltd, Ergates Industrial Area, 2643, Ergates, Nicosia, Cyprus

*corresponding author: tel.: +386 1 4773 552; fax: +386 1 25 19 385; e-mail:

albert.prodan@ijs.si

Abstract

Titanium borates show promising hydrogen storage characteristics. Structural relaxation around individual hydrogen atoms and the binding energies are studied by means of the density functional theory methods for a number of hydrogenated TiB_2 , TiB and Ti_2B structures. Starting with the possible symmetric hydrogen sites a random structure searching has been performed, in addition to locate all energetically stable adsorption sites. It is shown that for the three bulk compounds considered, the lowest binding energies are obtained for TiB_2 (in the 0.3-1.8 eV range), the largest for Ti_2B (in the 3.9-4.7 eV range), while for TiB they are intermediate (in the 2.8-3.5 eV range). Calculations performed on hydrogenated Ti_2B result in two energetically stable sites for two different starting environments, suggesting a possible soft mode solution.

Keywords

Ti₂B, TiB, TiB₂, H environment, structural relaxation

1. Introduction

Hydrogen represents with its high heating value a fuel of the future; it is environmentally friendly and regenerative. The main technological problem remains its storage and safe handling. Thus, searching for new storage methods and new materials represents a challenging research field¹⁻³. A variety of hydrogen sorbents are currently considered. These include metal-organic⁴⁻⁶ and covalent-organic frameworks^{7,8}, which show promising properties with regard to safe operation, fast kinetics and structural stability, but show at the same time a rather low adsorption energy for H₂ and consequently a relatively small storage capacity at room temperature and intermediate pressures^{9,10}. Therefore, there is a need for new materials, whose H₂ adsorption energy would be higher, i.e., between 20–40 kJ/mole¹¹. Higher H₂ binding energies were already achieved with sorbents decorated with transition-metals¹²⁻²⁸. It was proposed that transition-metals added to fullerenes (C₆₀ or C₄₈B₁₂) and carbon nanotubes^{13,16} represent hydrogen adsorbents with storage capacities as high as 8-9 wt%. Polymers decorated with transition-metals were also considered as promising hydrogen storage media²¹⁻²⁷. Recently, a high weight percentage of H₂ uptake with rapid kinetics at room temperature was reported for transition-metal

ethylene complexes, formed by laser ablation²⁸. All these studies suggested that light metals like titanium, embedded into suitable skeletons made of other light elements, might represent ideal media for H₂ absorption. While titanium is characterized by a large H₂ binding energy, it also encounters a problem; its atoms, decorated on various nanostructures, tend to cluster²⁹. Possible solutions include the usage of metals with weak metal–metal interactions or strong metal–supporter interactions³⁰, as well as possible enhancement of the metal–supporter interactions by means of incorporated defects³¹ or by a direct integration of metal atoms into appropriate skeletons^{32–35}.

On the other hand boron, being lighter in comparison with carbon, represents a very good candidate to form titanium complexes with promising hydrogen storage characteristics^{36–38}. Titanium-substituted closo-boranes³² and tubular TiB₂ structures, based on graphite-like intercalated layered structures³³, were suggested as promising candidates³⁴. It was shown that metal clustering can be avoided in calcium-doped boron fullerenes/nanotubes^{39,40}, where each calcium atom takes up as much as five H₂ molecules. In addition, several studies were performed on small boron clusters; it was shown that B_x clusters with x up to 20 prefer planar ordering^{41–45}. Such agglomerates also represent potential building blocks in complexes with polymers and transition-metals^{46–49}.

In the present work the hydrogenation as a function of the microstructural properties of TiB₂, TiB and Ti₂B is studied by means of the density functional theory (DFT) calculations, performed within the generalized-gradient-approximation functional and with the use of a plane-wave basis set. For each of the three compounds the possible hydrogen absorption sites are determined by considering the most likely interstitial positions with high coordination and, additionally, by ab-initio random structure searching studies⁵⁰, which give the minimum energy configurations for randomly chosen initial hydrogen sites. This approach is not only useful for finding absorption sites which are not expected on the basis of chemical intuition, but also for a rough estimation of the “basins of attraction” for the potential-energy-surface (PES) minima. Both can provide some information on the possible hydrogen diffusion pathways. Structural relaxation in the vicinity of the hydrogen absorption sites is studied by performing the calculations in enlarged super-cells.

In Sec. 2 we discuss the TiB_x structures, provide the crystallographic data and list the a-priori absorption sites for the hydrogen atoms. In Sec. 3 the structural relaxation and the corresponding binding energies in the presence of hydrogen defects are presented. We conclude with a discussion on the relevance of our results for the practical aspects of hydrogen storage in the TiB_x compounds.

2. The TiB_x structures

2.1. The titanium di-boride TiB₂

TiB₂ crystallizes in the *AlB₂* or *β-ThSi₂* structure type^{51,52}. The structure is shown in *Fig. 1* and the corresponding crystallographic data are given in *Table 1*. Four possible ideal H positions, given in the table with bold figures, are considered further. These positions are illustrated in *Fig. 1b*.

Table 1

Crystallographic data of TiB₂ with four possible ideal H positions:
space group: P6/mmm (no. 191)
a = 0.3023 nm, c = 0.3220 nm

<i>atom</i>	<i>Wyckoff</i>	<i>x</i>	<i>y</i>	<i>z</i>
-------------	----------------	----------	----------	----------

Ti	1a	0	0	0
B	2d	1/3	2/3	1/2
H1	2c	2/3	1/3	0
H2	6i	0	1/2	1/4
H3	1b	0	0	1/2
H4	6k	4/5	0	1/2

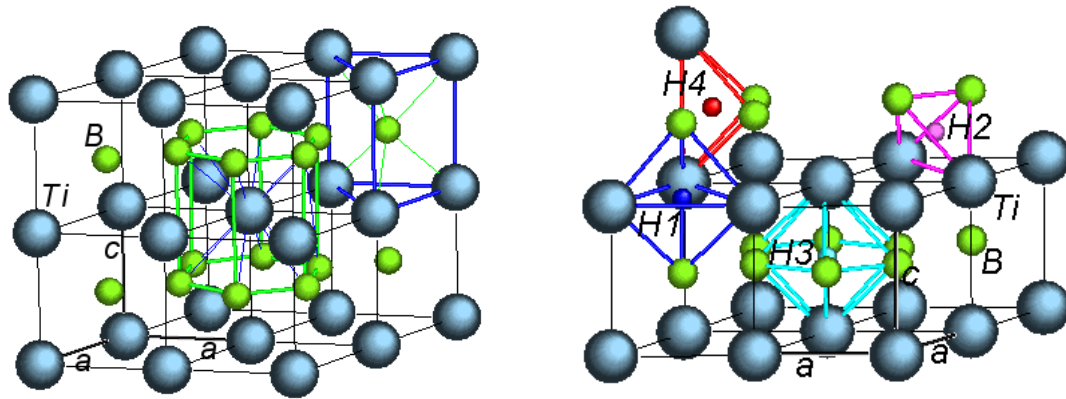


Fig.1 The structure of TiB_2 with the medium (green) balls representing B atoms in the trigonal prismatic coordination with Ti and the larger Ti atoms centered in 12-coordinated hexagonal prismatic coordination with B atoms (a). The small (dark blue, violet, light blue and red) balls represent the four H ideal positions, listed in *Table 1* (b).

The ideal coordination of the H1 position is trigonal bipyramidal within two H-B distances of 0.161 nm and three H-Ti bonds of 0.175 nm. The B-H-B vertex is parallel to the c -axis, while the three Ti atoms form a triangle perpendicular to the c -axis with the H atom in the middle. The H2 positions are surrounded by a deformed tetrahedron with two H-B bonds of 0.119 nm and two H-Ti bonds of 0.171 nm. The 2-fold axis of the tetrahedron is parallel to the TiB_2 c -axis. Six of such tetrahedra share faces with the H1 polyhedra. The ideal H3 position is coordinated by six B atoms at 0.175 nm and two Ti atoms at 0.161 nm. The TiB_2 c -axis is parallel to the Ti-H-Ti vertex and perpendicular to the B hexagon. The H4 positions are centered in deformed tetrahedra with two H-B bonds of 0.126 nm and two H-Ti bonds of 0.172 nm. Six of these tetrahedra compose into the enlarged H3 polyhedron.

2.2. The titanium mono-boride TiB

The mono-boride TiB crystallizes in the FeB structure type^{51,53,54}. The structure is shown in *Fig.2* and the corresponding crystallographic data are given in *Table 2*. The structure is obtained from the one of TiB_2 by removing from it every second trigonal prism. The remaining prisms form columns along the new orthorhombic b -direction. The structural tunnels thus formed collapse

with the remaining trigonal prisms and change their coordination into single-capped trigonal prismatic. The symmetry is accordingly reduced from hexagonal into orthorhombic. There are eight possible nonrelated H positions, three (H4, H7 and H8) in the more general (8d) and the remaining five (H1, H2, H3, H5 and H6) in (4c) positions. As shown below, four of these (H1, H3, H5 and H6) are energetically stable, while the others do not correspond to a PES minimum. Only the H1 positions are coordinated with four Ti atoms; these tetrahedra are edge-connected and form zig-zag chains along the orthorhombic *b*-direction. The remaining H positions are in 1B3Ti coordinations, except of H7 and H8, which occupy deformed 2B2Ti tetrahedra.

Table 2

Crystallographic data of the *TiB* structure with eight possible H positions; positions shown in bold are the energetically stable positions:

space group: Pnma (no. 62)

$a = 0.6120$ nm, $b = 0.3060$ nm, $c = 0.4560$ nm

<i>atom</i>	<i>Wyckoff</i>	<i>x</i>	<i>y</i>	<i>z</i>
Ti	(4c)	0.18000	1/4	1/8
B	(4c)	0.03600	1/4	0.61000
H1	(4c)	22/25	1/4	0.07300
H2	(4c)	0.78600	3/4	0.50370
H3	(4c)	12/25	1/4	0.63000
H4	(8d)	0.598	1/2	0.69125
H5	(4c)	0.286	3/4	0.24625
H6	(4c)	0.661	3/4	0.15625
H7	(8d)	0.535	5/8	0.8475
H8	(8d)	0.866	0	9/16

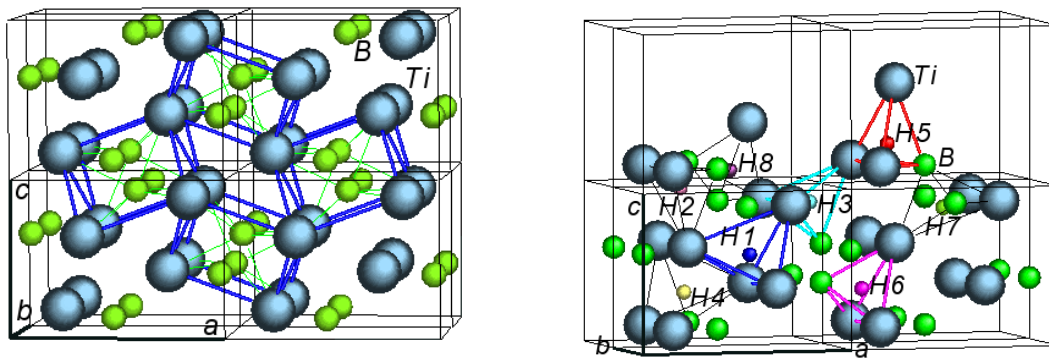


Fig.2 The structure of *TiB* with the medium (green) and large (blue) balls representing B and Ti atoms (a). Small balls (of different colors) represent possible H positions, listed in *Table 2* with the corresponding bold (colored) tetrahedra representing the non-related stable interstices (b).

2.3. The titanium semi-boride Ti_2B

Ti_2B crystallizes in the $\theta-Al_2Cu$ structure type⁵⁵⁻⁵⁷. The structure is shown in Fig. 3a and the relevant crystallographic data are collected in Table 1. By removing half of the tetragonal antiprismatic columns the structure type of $NbTe_4/TaTe_4$ is obtained. From the three unrelated H positions, given in Table 3 and shown in Fig. 3b, only two, i.e. H1 in 4Ti coordination and the two equivalent H3 sites in 3Ti1B coordination, were found to be energetically stable.

Table 3

Crystallographic data of the Ti_2B structure with the three symmetry unrelated ideal H positions; the two positions shown in bold are the energetically stable ones.

space group: I4/mcm (no.140)
a = 0.564 nm, c = 0.475 nm

atom	Wyckoff	x	y	z
B	4a	0	0	1/4
Ti	8h	1/6	1/3	0
H1	16l	1/8	5/8	13/16
H2	4c	0	0	0
H3a*	16l	5/12	17/24	11/16
H3b*	16l	1/12	5/24	5/16

*32 equivalent H3 sites are represented by two sets of symmetry-related 16l Wyckoff positions.

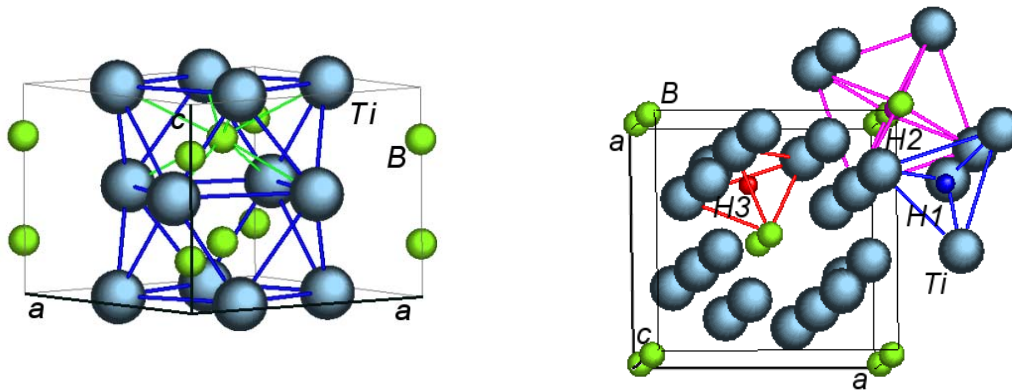


Fig. 3 The crystal structure of Ti_2B with B atoms, represented by the middle sized (green) balls, in tetragonal anti-prismatic coordination with Ti atoms, represented by the large (blue) balls (a). Small (dark blue, violet and red) balls represent the hydrogen H1 (4Ti), H2 (4Ti₂B) and H3 (3Ti1B) environments (b).

3. The relaxation of the unit-cells and the atomic positions

The calculations were performed using the plane-wave DFT code PWSCF (part of the Quantum Espresso package)⁵⁸ with the generalized gradient approximation (GGA) PBE functional⁵⁹. Ultrasoft pseudopotentials with 400 Ry cutoff for the charge density and 40 Ry cutoff for the kinetic energy were used⁶⁰. A 8x8x8 or 4x4x4 (dependent on the super-cell size) Monkhorst-Pack mesh of k-points was used with a cold-smearing by 0.02 Ry^{61,62}.

The experimental crystallographic data were used as the starting points for both, the relaxation of the unit cell and the relaxation of all atomic positions. This preliminary step was performed to test both, the experimental data and the numerical method used. The convergence threshold for the total energy was 0.5 meV and the threshold for forces was 10 meV/Å. The symmetry was not enforced during the minimization process, although in all cases considered no significant symmetry distortion took place.

Two series of calculations have been performed for each TiB_x compound. In the first series the H atom was initially placed at one of the a-priori high-symmetry positions inside the cell, and then the whole structure was relaxed. For stable H positions, the relaxation of the H atom was always found to be relatively small. For unstable H positions, the H position was, however, displaced in the direction of the potential-energy-surface gradient until reaching the nearest local minimum. This first series of calculations already gave good indication about the possible H binding sites. Nevertheless, such a-priori initial positions based on chemical intuition are, in principle, subject to bias, since non-intuitive binding scenarios are not excluded. For this reason, we complemented this series of calculation by an additional one, where fully random (arbitrary) initial H positions were chosen. The relaxation calculations themselves were then performed in the same way as in the first series. This kind of studies are also known as the “ab-initio random structure searching”. As detailed in the following, For TiB₂ and TiB no new solutions were found, thus the value of performing the random structure searching was mainly in establishing the size of the basins of attraction for various local PES minima (the lowest energy solution, i.e., global minima, also tend to correspond to the solutions with the largest basins of attraction). For Ti₂B, however, random structure searching established the existence of pairs of solutions with similar energy, suggesting the presence of a soft mode in the system. The occurrence of this phenomenon would likely go undetected without the random structure search.

3.1. TiB₂

In accord with literature^{51,52} the TiB₂ lattice parameters, obtained by GGA calculations, are $a = 0.3026$ nm and $c = 0.3212$ nm. To reduce the finite-size effects, calculations with H atoms in different environments have been performed in a ($2a \times 2a \times 2c$) super-cell with 8 Ti and 16 B atoms. The results are collected in *Table 4* and the relaxed environments of the possible four H interstices are shown in *Fig. 4*. The binding energy E_{bind} is defined as the difference between the total energy of the TiB₂ cell containing one H atom and the sum of the energy of the pure TiB₂ cell and the energy of one H atom in empty space. By comparing the binding energies calculated for a ($2a \times 2a \times 2c$) super-cell with those for a ($1a \times 1a \times 1c$) cell, we found differences of the order of one percent, which was much less than the differences in E_{bind} for different PES minima. The results indicate that the calculations may safely be performed in the eight times smaller cell and that the structural relaxation is small and of a very short range.

Table 4

Relaxed super-cell parameters, binding energies and atomic positions of either of the four H, eight Ti and sixteen B positions in the primitive ($2a \times 2b \times 2c$) TiB₂ super-cell. The Ti (0, 0, 0) position was kept in all cases fixed during the relaxation.

unit cells:

H1: a = 0.60774 nm, b = 0.60774 nm, c = 0.64267 nm, $\alpha = 89.9991^\circ$, $\beta = 89.9999^\circ$, $\gamma = 119.999^\circ$;
H2: a = 0.60728 nm, b = 0.60864 nm, c = 0.64491 nm, $\alpha = 90.0003^\circ$, $\beta = 90.0002^\circ$, $\gamma = 120.073^\circ$;
H3: a = 0.60671 nm, b = 0.60671 nm, c = 0.64756 nm, $\alpha = 90.0001^\circ$, $\beta = 89.9998^\circ$, $\gamma = 120.000^\circ$;
H4: a = 0.60734 nm, b = 0.60735 nm, c = 0.64664 nm, $\alpha = 89.9997^\circ$, $\beta = 90.0005^\circ$, $\gamma = 120.000^\circ$;

binding energies:

$E_{\text{bind}}(\text{H1}) = 1.79 \text{ eV}$; $E_{\text{bind}}(\text{H2}) = 1.28 \text{ eV}$; $E_{\text{bind}}(\text{H3}) = 0.26 \text{ eV}$; $E_{\text{bind}}(\text{H4}) = 0.51 \text{ eV}$.

<i>atom</i>	<i>starting positions</i>			<i>relaxed positions (H1)</i>			<i>relaxed positions (H2)</i>		
	<i>x</i>	<i>y</i>	<i>z</i>	<i>x</i>	<i>y</i>	<i>z</i>	<i>x</i>	<i>y</i>	<i>z</i>
Ti	0	0	0	0.0000	0.0000	0.0000	0.0000	0.0000	0.0000
B	1/6	1/3	1/4	0.1716	0.3383	0.2544	0.1751	0.3479	0.2650
B	1/3	1/6	1/4	0.3399	0.1700	0.2548	0.3335	0.1760	0.2548
Ti	0	0	1/2	0.0062	0.0031	0.5001	0.0000	0.0106	0.5041
B	1/6	1/3	3/4	0.1729	0.3370	0.7495	0.1670	0.3438	0.7522
B	1/3	1/6	3/4	0.3399	0.1700	0.7447	0.3335	0.1775	0.7539
Ti	0	1/2	0	0.0066	0.5033	0.0010	0.0000	0.5207	0.0000
B	1/6	5/6	1/4	0.1716	0.8334	0.2544	0.1668	0.8438	0.2549
B	1/3	2/3	1/4	0.3399	0.6700	0.2514	0.3335	0.6783	0.2548
Ti	0	1/2	1/2	0.0066	0.5033	0.5013	0.0000	0.5102	0.5041
B	1/6	5/6	3/4	0.1729	0.8360	0.7495	0.1678	0.8442	0.7515
B	1/3	2/3	3/4	0.3398	0.6699	0.7497	0.3335	0.6767	0.7539
Ti	1/2	0	0	0.5099	0.0000	0.0000	0.4989	0.0098	0.0036
B	2/3	1/3	1/4	0.6765	0.3383	0.2544	0.6665	0.3448	0.2548
B	5/6	1/6	1/4	0.8399	0.1700	0.2514	0.8249	0.1729	0.2650
Ti	1/2	0	1/2	0.5068	0.0031	0.5001	0.4975	0.0091	0.5058
B	2/3	1/3	3/4	0.6739	0.3369	0.7495	0.6665	0.3432	0.7539
B	5/6	1/6	3/4	0.8400	0.1701	0.7497	0.8330	0.1769	0.7522
Ti	1/2	1/2	0	0.5099	0.5099	0.0000	0.5011	0.5109	0.0036
B	2/3	5/6	1/4	0.6733	0.8366	0.2515	0.6665	0.8424	0.2548
B	5/6	2/3	1/4	0.8399	0.6700	0.2514	0.8332	0.6770	0.2549
Ti	1/2	1/2	1/2	0.5068	0.5037	0.5001	0.5025	0.5116	0.5058
B	2/3	5/6	3/4	0.6733	0.8366	0.7486	0.6665	0.8440	0.7539
B	5/6	2/3	3/4	0.8400	0.6699	0.7497	0.8322	0.6765	0.7515
H1	1/3	1/6	0	0.3398	0.1699	0.0310			
H2	0	1/4	1/8				0.0000	0.2604	0.1033

<i>atom</i>	<i>starting positions</i>			<i>relaxed positions (H3)</i>			<i>relaxed positions (H4)</i>		
	<i>x</i>	<i>y</i>	<i>z</i>	<i>x</i>	<i>y</i>	<i>z</i>	<i>x</i>	<i>y</i>	<i>z</i>
Ti	0	0	0	0.0000	0.0000	0.0000	0.0000	0.0000	0.0000
B	1/6	1/3	1/4	0.1685	0.3371	0.2606	0.1623	0.3332	0.2507
B	1/3	1/6	1/4	0.3371	0.1685	0.2606	0.3325	0.1768	0.2507
Ti	0	0	1/2	0.0000	0.0000	0.5212	0.0000	0.0000	0.5014
B	1/6	1/3	3/4	0.1675	0.3350	0.7606	0.1680	0.3333	0.7507
B	1/3	1/6	3/4	0.3350	0.1675	0.7606	0.3340	0.1668	0.7507
Ti	0	1/2	0	0.0000	0.5000	0.0112	0.0005	0.5005	0.0003
B	1/6	5/6	1/4	0.1685	0.8315	0.2606	0.1558	0.8233	0.2507
B	1/3	2/3	1/4	0.3333	0.6667	0.2606	0.3322	0.6618	0.2507

Ti	0	1/2	1/2	0.0000	0.5000	0.5100	0.0005	0.5005	0.5011
B	1/6	5/6	3/4	0.1675	0.8325	0.7606	0.1672	0.8332	0.7507
B	1/3	2/3	3/4	0.3333	0.6667	0.7606	0.3338	0.6656	0.7507
Ti	1/2	0	0	0.5000	0.0000	0.0112	0.5041	0.0000	0.0083
B	2/3	1/3	1/4	0.6667	0.3333	0.2606	0.6704	0.3382	0.2507
B	5/6	1/6	1/4	0.8315	0.1685	0.2606	0.8327	0.1666	0.2507
Ti	1/2	0	1/2	0.5000	0.0000	0.5100	0.5041	0.0000	0.5096
B	2/3	1/3	3/4	0.6667	0.3333	0.7606	0.6682	0.3344	0.7507
B	5/6	1/6	3/4	0.8325	0.1675	0.7606	0.8362	0.1677	0.7507
Ti	1/2	1/2	0	0.5000	0.5000	0.0112	0.5000	0.4995	0.0003
B	2/3	5/6	1/4	0.6629	0.8315	0.2606	0.6662	0.8334	0.2507
B	5/6	2/3	1/4	0.8315	0.6629	0.2606	0.8292	0.6668	0.2507
Ti	1/2	1/2	1/2	0.5000	0.5000	0.5100	0.5000	0.4995	0.5011
B	2/3	5/6	3/4	0.6650	0.8325	0.7606	0.6685	0.8324	0.7507
B	5/6	2/3	3/4	0.8325	0.6650	0.7606	0.8347	0.6668	0.7507
H3	0	0	1/4	0.0000	0.0000	0.2606			
H4	2/5	0	1/4				0.4031	0.0001	0.2507

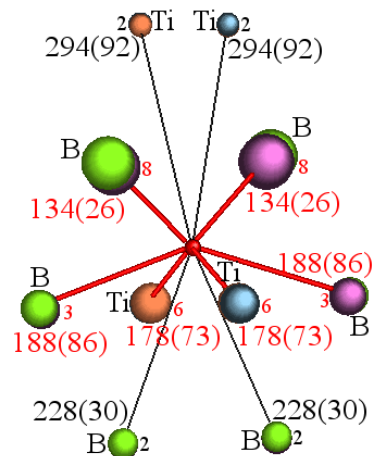
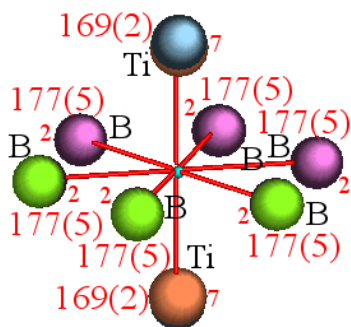
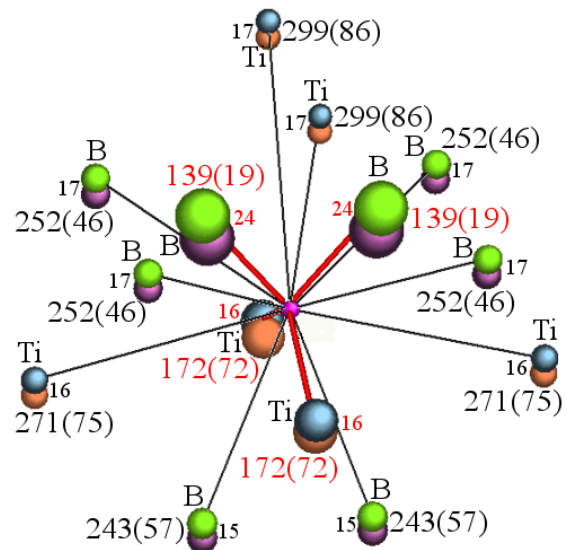
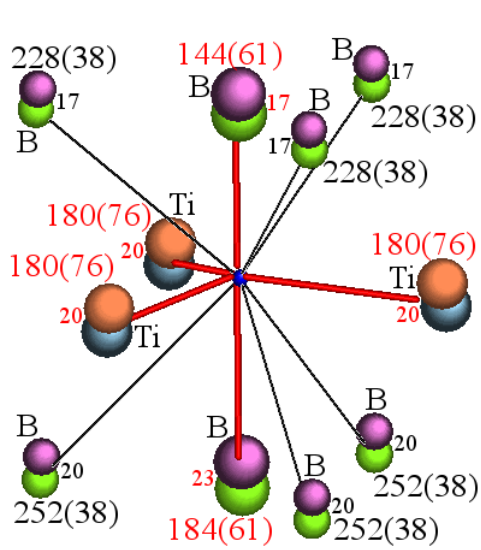


Fig.4 The relaxed neighbourhood of the a) H1 (small and dark blue), b) H2 (small and violete), c) H3 (small and light blue) and d) H4 (small and red) atoms in the TiB_2 structure. The sizes of the marked Ti (dark blue original and orange relaxed) and B (green original and violete relaxed) atoms are proportional to the reciprocal values of their distances from the H atom considered. The distances from the H atoms to the nearest displaced (bold and red) and second nearest displaced (light and black) atoms are given with large figures in $10^{-3} \times \text{nm}$ (the last figures of the undisplaced positions in brackets). The corresponding small figures give the displacements in the same units. All atoms within 0.3 nm from the H atom are shown.

3.2. TiB

Structural relaxation within the GGA approach gives in case of pure TiB unit cell parameters ($a = 0.610 \text{ nm}$, $b = 0.304 \text{ nm}$ and $c = 0.455 \text{ nm}$) and atomic positions for Ti (0.1775 1/4 0.1225) and B (0.0302 1/4 0.59), which are in good agreement with the values from the literature^{51,53,54}, listed in *Table 2*. Calculations with an additional H atom in one of the four possible positions have been performed within the basic unit cell ($1\mathbf{a} \times 1\mathbf{b} \times 1\mathbf{c}$) with four Ti and four B atoms. The results are collected in *Table 5* and the local environments of the H atoms are shown in *Fig. 5*.

Table 5

Relaxed unit cell parameters, binding energies and atomic positions of either of the four H, four Ti and four B positions within a primitive ($1\mathbf{a} \times 1\mathbf{b} \times 1\mathbf{c}$) TiB unit cell. The Ti (0.18, 1/4, 1/8) position was in all cases kept fixed during the relaxation.

unit cells:

H1: $a = 0.61031 \text{ nm}$, $b = 0.30539 \text{ nm}$, $c = 0.46103 \text{ nm}$, $\alpha = 90.000^\circ$, $\beta = 89.573^\circ$, $\gamma = 90.000^\circ$;

H3: $a = 0.61577 \text{ nm}$, $b = 0.30618 \text{ nm}$, $c = 0.45844 \text{ nm}$, $\alpha = 90.000^\circ$, $\beta = 90.411^\circ$, $\gamma = 90.000^\circ$;

H5: $a = 0.61238 \text{ nm}$, $b = 0.30597 \text{ nm}$, $c = 0.46161 \text{ nm}$, $\alpha = 90.000^\circ$, $\beta = 89.616^\circ$, $\gamma = 90.000^\circ$;

H6: $a = 0.60855 \text{ nm}$, $b = 0.30762 \text{ nm}$, $c = 0.46151 \text{ nm}$, $\alpha = 90.000^\circ$, $\beta = 90.205^\circ$, $\gamma = 90.000^\circ$;

binding energies:

$E_{\text{bind}}(\text{H1}) = 3.54 \text{ eV}$; $E_{\text{bind}}(\text{H3}) = 3.20 \text{ eV}$; $E_{\text{bind}}(\text{H5}) = 2.98 \text{ eV}$; $E_{\text{bind}}(\text{H6}) = 2.77 \text{ eV}$.

atom	starting positions			relaxed positions (H1)			relaxed positions (H3)		
	x	y	z	x	y	z	x	y	z
Ti	0.18	1/4	1/8	0.18	1/4	1/8	0.18	1/4	1/8
Ti	17/25	1/4	3/8	0.6778	1/4	0.3792	0.6920	1/4	0.3691

Ti	0.82	3/4	7/8	0.8206	3/4	0.8722	0.8306	3/4	0.8776
Ti	8/25	3/4	5/8	0.3257	3/4	0.6254	0.3187	3/4	0.6230
B	0.036	1/4	0.61	0.0329	1/4	0.5961	0.0324	1/4	0.6001
B	0.536	1/4	0.89	0.5248	1/4	0.9008	0.5331	1/4	0.9159
B	0.464	3/4	0.11	0.4713	3/4	0.0995	0.4745	3/4	0.0958
B	0.964	3/4	0.39	0.9767	3/4	0.4165	0.9752	3/4	0.4011
H1	22/25	1/4	0.073	0.8795	1/4	0.0722			
H3	12/25	1/4	0.63				0.4733	1/4	0.6300

atom	starting positions			relaxed positions (H5)			relaxed positions (H6)		
	x	y	z	x	y	z	x	y	z
Ti	0.18	1/4	1/8	0.18	1/4	1/8	0.18	1/4	1/8
Ti	17/25	1/4	3/8	0.6908	1/4	0.3869	0.6787	1/4	0.3887
Ti	0.82	3/4	7/8	0.8352	3/4	0.8830	0.8301	3/4	0.8711
Ti	8/25	3/4	5/8	0.3322	3/4	0.6387	0.3256	3/4	0.6264
B	0.036	1/4	0.61	0.0394	1/4	0.6044	0.0315	1/4	0.5964
B	0.536	1/4	0.89	0.5396	1/4	0.9090	0.5274	1/4	0.8936
B	0.464	3/4	0.11	0.4920	3/4	0.0953	0.4671	3/4	0.0924
B	0.964	3/4	0.39	0.9779	3/4	0.4126	0.9777	3/4	0.4039
H5	0.286	3/4	0.24625	0.3120	3/4	0.2472			
H6	0.661	3/4	0.15625				0.6730	3/4	0.2072

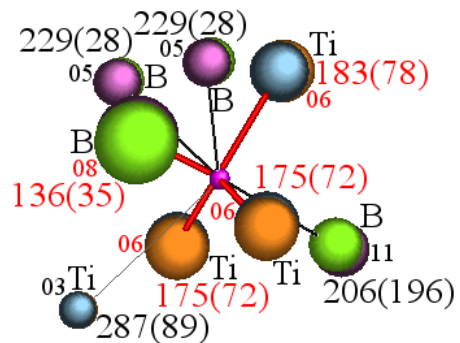
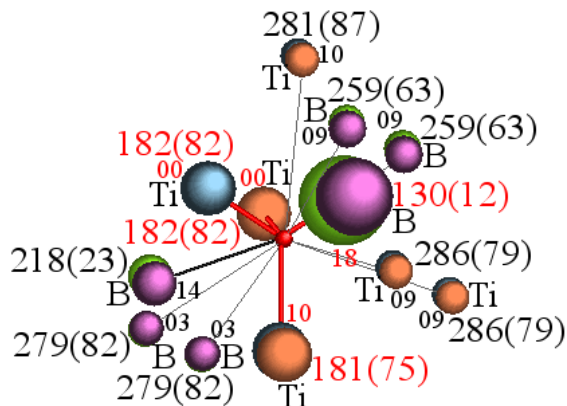
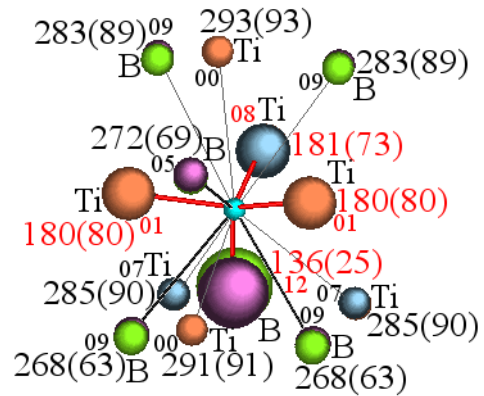
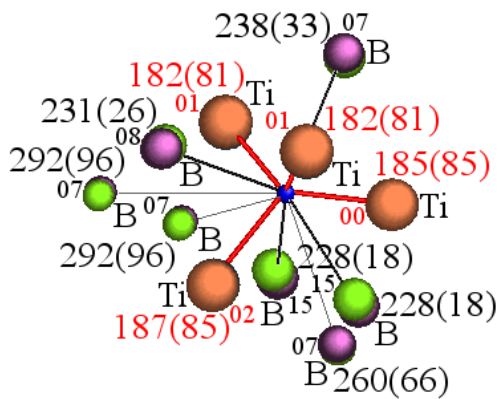


Fig.5 The relaxed neighbourhood of the a) H1 (small and dark blue), b) H3 (small and light blue), c) H5 (small and red) and d) H6 (small and violete) atoms in the TiB structure. The sizes of the marked Ti (dark blue original and orange relaxed) and B (green original and violete relaxed) atoms are proportional to the reciprocal values of their distances from the H atoms considered. The distances from the H atoms to the nearest displaced (bold and red) and second nearest displaced (middle, light and black) atoms are given with large figures in $10^{-3} \times \text{nm}$ (the last figures of the undisplaced positions in brackets). The corresponding small figures give the relaxed displacements in the same units. Shown are all atoms within 0.3 nm from the H atoms.

3.3. Ti_2B

The relaxed parameters ($a = 0.564 \text{ nm}$ and $c = 0.475 \text{ nm}$), obtained by GGA calculations for the pure tetragonal body-centered Bravais lattice of Ti_2B are again in accord with the data from the literature^{55,56}. The same unit cell with eight Ti and four B atoms was then used in calculations with additional individual H atoms. The relaxed unit cell parameters and atomic positions, which correspond to the original values listed in *Table 3*, are given in *Table 6* together the corresponding binding energies. The original H2 position was found to be energetically unstable. Two slightly different stable arrangements were found for each of the remaining two H environment. These are shown in *Fig. 6* and marked as H1a and H1b for the H1 position in the tetrahedral 4Ti environment and as H3a and H3b for the H3 position in the 3Ti1B coordination.

Table 6

Relaxed positions of one H (H1a, H1b, H3a or H3b), eight Ti and four B positions in the body-centered Ti_2B unit cell. The B (0, 0, 1/4) position was in all cases kept fixed during relaxation.

unit cells:

H1a: $a = 0.5622 \text{ nm}$, $b = 0.5665 \text{ nm}$, $c = 0.4803 \text{ nm}$, $\alpha = 89.94^\circ$, $\beta = 89.80^\circ$, $\gamma = 88.82^\circ$;

H1b: $a = 0.5709 \text{ nm}$, $b = 0.5709 \text{ nm}$, $c = 0.4738 \text{ nm}$, $\alpha = 90.04^\circ$, $\beta = 90.04^\circ$, $\gamma = 90.22^\circ$;

H3a: $a = 0.5669 \text{ nm}$, $b = 0.5632 \text{ nm}$, $c = 0.4795 \text{ nm}$, $\alpha = 89.81^\circ$, $\beta = 90.47^\circ$, $\gamma = 89.69^\circ$;

H3b: $a = 0.5724 \text{ nm}$, $b = 0.5691 \text{ nm}$, $c = 0.4733 \text{ nm}$, $\alpha = 90.01^\circ$, $\beta = 90.23^\circ$, $\gamma = 90.28^\circ$;

binding energies:

$E_{\text{bind}}(\text{H1a}) = 4.66 \text{ eV}$, $E_{\text{bind}}(\text{H1b}) = 4.16 \text{ eV}$, $E_{\text{bind}}(\text{H3a}) = 4.25 \text{ eV}$ and $E_{\text{bind}}(\text{H3b}) = 3.88 \text{ eV}$.

atom	starting positions			relaxed positions (H1a)			relaxed positions (H1b)		
	x	y	z	x	y	z	x	y	z
B	0	0	1/4	0	0	1/4	0	0	1/4
B	1/2	1/2	1/4	0.4947	0.4931	0.1189	0.4939	0.5069	0.2502
Ti	1/6	1/3	0	0.1511	0.3186	0.9344	0.1696	0.3385	0.0530
B	0	0	3/4	0.9988	0.9935	0.6214	0.9976	0.0068	0.8556
B	1/2	1/2	3/4	0.5003	0.4963	0.7515	0.5004	0.5040	0.8557
Ti	2/3	1/6	0	0.6757	0.1466	0.9373	0.6575	0.1640	0.0485
Ti	5/6	2/3	0	0.8456	0.6698	0.9341	0.8322	0.6759	0.0528
Ti	1/3	5/6	0	0.3220	0.8433	0.9359	0.3342	0.8408	0.0510
Ti	5/6	1/3	1/2	0.8147	0.3339	0.4386	0.8315	0.3378	0.5526
Ti	1/3	1/6	1/2	0.3410	0.1718	0.4331	0.3311	0.1725	0.5543

Ti	1/6	2/3	1/2	0.1880	0.6494	0.4380	0.1666	0.6730	0.5496
Ti	2/3	5/6	1/2	0.6516	0.8259	0.4408	0.6662	0.8375	0.5541
H1a	7/8	5/8	5/16	0.8862	0.6192	0.3097			
H1b	7/8	3/8	3/16				0.8754	0.3816	0.1753

atom	starting positions			relaxed positions (H3a)			relaxed positions (H3b)		
	x	y	z	x	y	z	x	y	z
B	0	0	1/4	0	0	1/4	0	0	1/4
B	1/2	1/2	1/4	0.4960	0.4990	0.1215	0.5000	0.5042	0.2495
Ti	1/6	1/3	0	0.1495	0.3185	0.9364	0.1628	0.3426	0.0538
B	0	0	3/4	0.9994	0.9960	0.6214	0.9995	0.0114	0.8628
B	1/2	1/2	3/4	0.4954	0.4882	0.7535	0.5020	0.5045	0.8589
Ti	2/3	1/6	0	0.6759	0.1486	0.9356	0.6616	0.1669	0.0570
Ti	5/6	2/3	0	0.8468	0.6721	0.9350	0.8384	0.6587	0.0648
Ti	1/3	5/6	0	0.3159	0.8490	0.9501	0.3442	0.8451	0.0547
Ti	5/6	1/3	1/2	0.8195	0.3427	0.4365	0.8308	0.3357	0.5558
Ti	1/3	1/6	1/2	0.3440	0.1714	0.4373	0.3320	0.1726	0.5530
Ti	1/6	2/3	1/2	0.1656	0.6471	0.4270	0.1825	0.6646	0.5432
Ti	2/3	5/6	1/2	0.6615	0.8241	0.4223	0.6604	0.8363	0.5444
H3a	5/12	17/24	11/16	0.4297	0.7008	0.6440			
H3b	11/12	19/24	11/16				0.9408	0.8040	0.7451

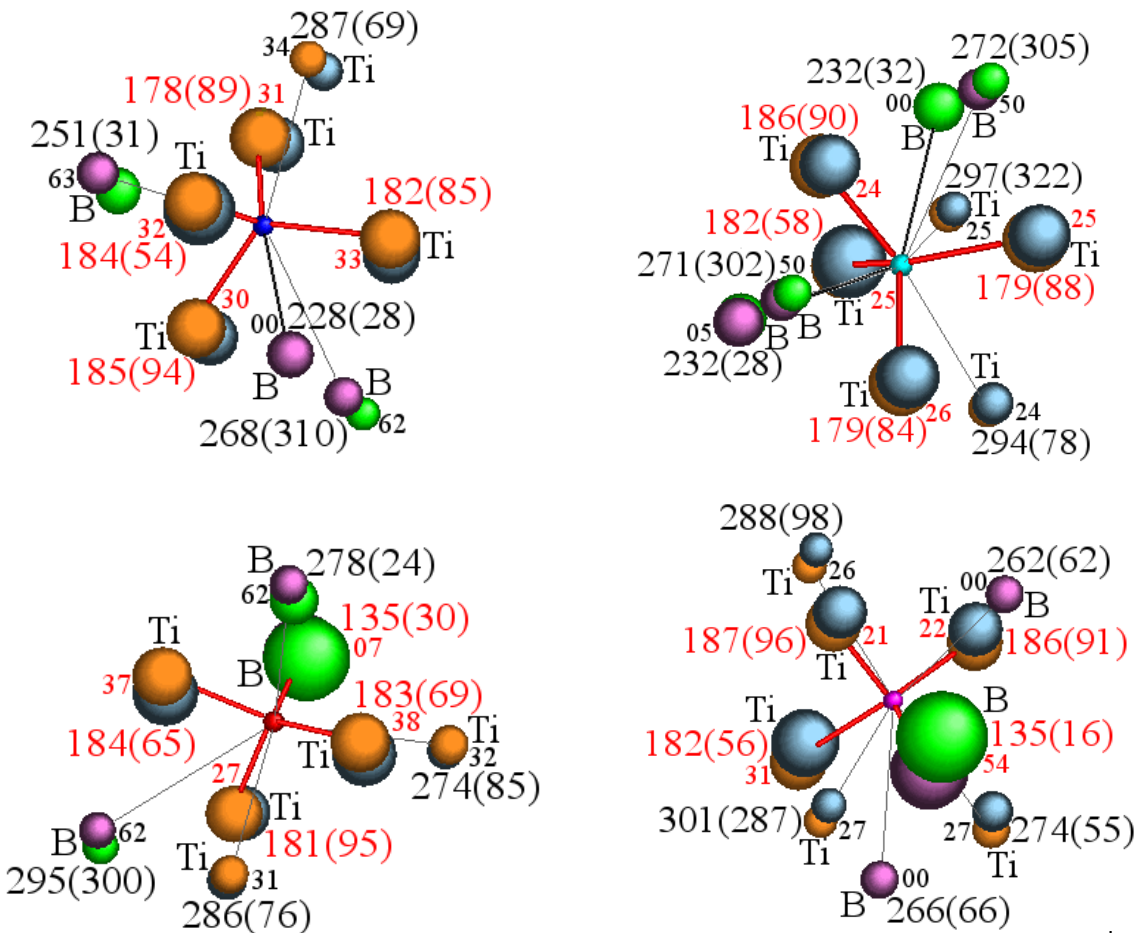


Fig.6 The relaxed neighbourhoods of the a) H1a (small and dark blue), b) H1b (small and light blue), c) H3a (small and red) and d) H3b (small and violete) atomic positions in the Ti_2B structure. The sizes of the Ti (dark blue original and orange relaxed) and B (green original and violete relaxed) atoms are proportional to the reciprocal values of their distances from the H atoms. The distances from the H atoms to the nearest displaced (bold and red) and second nearest displaced (middle, light and black) atoms are given with large figures in $10^{-3} \times \text{nm}$ (the last figures of the undisplaced positions in brackets). The corresponding small figures show the displacements in the same units. All atoms within a sphere with a radius slightly larger than 0.3 nm from the H atoms are shown.

4. Discussion

It was shown recently³⁴ that metal diborides, particularly in the form of nanotubes, represent very promising H storage media with molecular H_2 binding energies in the range of 0.2 to 0.6 eV/ H_2 and a very high theoretical retrievable H_2 storage density (of the order of almost 8 wt %). The binding energies of individual H atoms, obtained in our calculations, are in range of 0.26 eV to 1.78 eV for TiB_2 , while the binding energies obtained in case of the other two hydrogenated compounds, i.e. the mono- and semi-borides, appear much higher; for the four hydrogenated Ti mono-borides the H binding energies fall between 2.77 eV and 3.54 eV and for the semi-borides even higher, between 3.88 eV and 4.66 eV. However, direct comparisons of these values with regard to possible hydrogen storage are not possible. First of all, as hydrogen storage media compounds are desired, able to absorb larger amounts of hydrogen, while in our calculations single H atoms and their environments were considered. Also, the energy obtained for a H_2 molecule has to be replaced in case of a free H atom by the dissociative energy of the molecule in vacuum (4.48 eV)⁶³. It was shown recently⁶⁴ that relevant for hydrogen storage are compounds with changes in enthalpy between 30 and 70 kJ/mole H_2 , which corresponds to H binding energies between 2.4 and 2.7 eV/H atom. These values would roughly correspond to those obtained for the hydrogenated TiB compounds.

The structural adjustment required by the presence of the H atom was found to be in most cases small, with only the first neighbours displaced appreciably. However, a certain minor influence of the next, periodically positioned H atom onto the next-nearest metal atoms cannot be completely excluded. To show that this influence is small, the initial calculations (on the TiB_2 -based structures) were performed in enlarged super-cells. The remaining calculations (on TiB - and Ti_2B -based structures) were performed with the basic unit cells only; this made it possible to perform random structure search calculations with more initial starting positions for the H atom. The random structure search was performed for a few tens of individual positions for each compound considered. It is thus very likely that we have located all PES minima. We also observe that the H adsorption sites with a strong binding correspond to large bassins of attraction in the position space.

Typical ionic hydrides are binary alkali-metal hydrides (e.g. LiH with the sodium chloride type of structure)⁶⁵ and alkaline-earth metal hydrides (e.g. MgH_2 with the rutile type of structure)⁶⁶, while most other complex metal hydrides⁶⁷ are characterized by mixed ionic/covalent bonding. A rather promising example with regard to H absorption/desorption kinetics is potassium aluminum hydride $KAlH_4$ with Al-H distances of about 0.165 nm⁶⁸. Contrary, interstitial hydrides are

characterized by metallic bonding. A well known example is Pd, whose face-centred cubic lattice parameter of 0.38874 nm is changed only slightly during hydrogenation, with Pd-H distances comparable to the Al-H distances in $KAlH_4$. The shortest Ti-H bonds in the three TiB_x compounds considered range between 0.170 and 0.185 nm, while the corresponding B-H distances are shorter, only between 0.130 and 0.135 nm. These compounds belong to the interstitial hydrides. They are lately intensively studied, because they show good hydrogenation and kinetic properties, particularly in the form of nanotubes and other low-dimensional forms^{34,69}.

4.1. TiB_2

As a result of the lattice relaxation around the H1 atom one of two B-H bonds is enlarged, while the second is shortened. Thus, the starting 3Ti2B H position is relaxed into an almost regular 3Ti1B tetrahedron with all three Ti-H and one B-H distances of about 0.18 nm. The remaining B-H bond is shorter (only 0.14 nm) and forms with the other four nearest neighbors a single-capped tetrahedron around the H1 atom. The next-nearest neighbors of H1 are only slightly accommodated to fit the relaxation.

The starting 2Ti2B coordination of the H2 atom is relaxed by enlarging the two nearest B-H distances symmetrically from 0.12 nm to 0.14 nm, while the nearest Ti-H bonds remain practically unchanged at 0.17 nm. Again, all remaining next-nearest Ti and B atoms are accordingly accommodated.

The H3 and H4 interstitial positions require only minor accommodation of the original TiB_2 structure. The relaxation of the H3 position hardly influences its starting 2Ti6B environment. Likewise, in case of H4 the rather deformed starting tetrahedrally-centered 2Ti2B coordination undergoes only a minor enlargement. The largest, but still relatively small displacements involve both nearest neighbor B-H bonds (0.13 nm), while the two nearest Ti-H bonds (0.18 nm) remain after relaxation only slightly shorter from the next-nearest B-H pairs (0.19 nm). Thus, the calculations clearly reveal that H3 and H4 are energetically stable positions within their respective original environments.

4.2. TiB

In case of the H1 atom, the four Ti-H bonds of the starting 4Ti tetragonal coordination undergo with relaxation only minor displacements. The calculations performed within the ($1a \times 1b \times 1c$) basic structure unit cell show that the next-nearest Ti and B positions are practically not affected by the relaxation.

The main relaxation around the H3 position involves a slight elongation of the shortest B-H bond (0.14 nm), while the three Ti-H bonds of the 3Ti1B tetrahedron remain practically unchanged (0.18 nm). Again, the second-nearest neighbors are hardly affected by the relaxation.

A very similar situation to the one of H3 takes place in case of both, the H5 and H6 atoms. Although slightly enlarged, the B-H bond of the 3Ti1B tetrahedron remains short (0.13 nm) in comparison with the remaining three Ti-H bonds (0.18 nm).

4.3. Ti_2B

In case of H1a and H1b the H atom is centered in an almost regular tetrahedral coordination with 4Ti atoms at the corners. As a result of relaxation, the four Ti-H bonds are in both cases only slightly modified. In case of H3a and H3b the two relaxations give again very similar results; both leave the three Ti-H bonds practically unchanged (0.18 nm), while the remaining B-H bond is only slightly enlarged (0.14 nm) and leaves the relaxed 3Ti1B tetrahedron deformed. In general, the displacements being the result of the relaxation, they appear somewhat larger than in TiB_2 and TiB . Thus, only the positions of the nearest neighbors to the H atom should be taken as

reliable, while the next-nearest Ti and B atoms seem to be appreciably influenced by the next-nearest H atoms. The two pairs of stable H positions correspond to two sets of relaxed unit-cell parameters; those obtained for H1a and H3a are similar and so are the parameters obtained for H1b and H3b atoms. This may suggest a soft-mode type of deformation with two stable solutions.

5. Conclusions

The following general conclusions follow from our numerical studies:

- The calculations show that the lattice relaxation caused by the presence of single H atoms in various TiB_2 , TiB and Ti_2B interstitial sites involves appreciably only the nearest environments of the H atoms.
- The binding energies of the H atoms are the lowest for the stable TiB_2 sites (between 0.26 eV and 1.78 eV), somewhat larger for the hydrogenated TiB compounds (between 2.77 eV and 3.54 eV) and the largest in case of Ti_2B (between 3.88 eV and 4.66 eV).
- Although direct comparisons with other calculations are applicable, the lattice relaxation and the corresponding binding energies obtained suggest that the Ti di-, mono- and semi-borides are promising candidates for hydrogen storage applications.
- The energetically stable coordination polyhedra around H sites include rather symmetrical 4Ti or 3Ti1B tetrahedra (the second with an additional single-capped shorter B-H bond), deformed 3Ti1B tetrahedral sites (with the only B-H bond appreciably shorter from the remaining three Ti-B bond), and very deformed 2Ti2B tetrahedra (with the pair of B-H bond much shorter from the remaining Ti-H pair).
- Two energetically stable sites were found for one environment in case of TiB_2 and for two such environments in case of Ti_2B . In the second case the four H positions with the corresponding two relaxed unit cells suggest a possible soft-mode solution.

Acknowledgments

Financial support of the Slovenian Research Agency (ARRS) (RŽ, HJPvM, EZ and AP), the bilateral cooperation program between the Hellenic Republic and the Republic of Slovenia (GSRT Code 043Γ) and the ATLAS-H2 European Project PIAP-GA-2009-251562 is gratefully acknowledged.

References

- [1] Ross D K. Hydrogen storage: The major technological barrier to the development of hydrogen fuel cell cars. *Vacuum* 2006; 80: 1084-9.
- [2] Züttel A. Hydrogen storage methods and materials. *Materials Today* 2003; Sept.: 24-33.
- [3] Crabtree GW, Dresselhaus MS. The hydrogen fuel alternative. *MRS Bulletin* 2008; 33: 421-8.
- [4] Roswell JLC, Yaghi OM. Strategies for hydrogen storage in metal-organic frameworks. *Angew Chem Int Edn* 2005; 44: 4670-9.
- [5] Collins DJ, Zhou H-C. Hydrogen storage in metal-organic frameworks. *J Mater Chem* 2007; 17: 3154-60.
- [6] Murray LJ, Dincă M, Long JR. Hydrogen storage in metal-organic frameworks. *Chem Soc Rev* 2009; 38: 1294-314
- [7] Han SS, Furukawa H, Yaghi OM, Goddard WA. Covalent Organic Frameworks as Exceptional Hydrogen Storage Materials. *J Am Chem Soc* 2008; 130: 11580-1.

- [8] Furukawa H, Yaghi OM. Storage of Hydrogen, Methane, and Carbon Dioxide in Highly Porous Covalent Organic Frameworks for Clean Energy Applications. *J Am Chem Soc* 2009; 131: 8875-83.
- [9] Wong-Foy AG, Matzger AJ, Yaghi OM. Exceptional H₂ Saturation Uptake in Microporous Metal-Organic Frameworks. *J Am Chem Soc* 2006; 128: 3494-5.
- [10] Garberoglio G. Computer Simulation of the Adsorption of Light Gases in Covalent Organic Frameworks. *Langmuir* 2007; 23: 12154-8.
- [11] Lochan RC, Head-Gordon M. Computational studies of molecular hydrogen binding affinities: The role of dispersion forces, electrostatics, and orbital interactions. *Phys Chem Chem Phys* 2006; 8: 1357-70.
- [12] Hamaed A, Trudeau M, Antonelli DM. H₂ Storage materials (22KJ/mol) using organometallic Ti fragments as σ -H₂ binding sites. *J Am Chem Soc* 2008; 130: 6992-9.
- [13] Zhao YF, Kim Y-H, Dillon AC, Heben MJ, Zhang SB. Hydrogen storage in novel organometallic buckyballs. *Phys Rev Lett* 2005; 94: 155504-1-4.
- [14] Durgun E, Ciraci S, Zhou W, Yildirim T. Transition-metal-ethylene complexes as high-capacity hydrogen-storage media. *Phys Rev Lett* 2006; 97: 226102-1-4.
- [15] Shin WH, Yang SH, Goddard WA, Kang JK. Ni-dispersed fullerenes: Hydrogen storage and desorption properties. *Appl Phys Lett* 2006; 88: 053111-1-3.
- [16] Yildirim T, Ciraci S. Titanium-decorated carbon nanotubes as a potential high-capacity hydrogen storage medium. *Phys Rev Lett* 2005; 94: 175501-1-4.
- [17] Durgun E, Jang YR, Ciraci S. Hydrogen storage capacity of Ti-doped boron-nitride and B/Be-substituted carbon nanotubes. *Phys Rev B* 2007; 76: 073413-1-4.
- [18] Mulfort KL, Hupp JT. Chemical reduction of metal-organic framework materials as a method to enhance gas uptake and binding. *J Am Chem Soc* 2007; 129: 9604-5.
- [19] Mavrandonakis A, Tylianakis E, Stubos AK, Froudakis GE. Why Li doping in MOFs enhances H₂ storage capacity? A multi-scale theoretical study. *J Phys Chem C* 2008; 112: 7290-4.
- [20] Han SS, Goddard WA. Lithium-doped metal-organic frameworks for reversible H₂ storage at ambient temperature. *J Am Chem Soc* 2007; 129: 8422-3.
- [21] Choi YJ, Lee JW, Choi JH, Kang JK. Ideal metal-decorated three dimensional covalent organic frameworks for reversible hydrogen storage. *Appl Phys Lett* 2008; 92: 173102-1-3.
- [22] Cooper AI, Poliakoff M. Hydrogen storage using polymer-supported organometallic dihydrogen complexes: a mechanistic study. *Chem Commun* 2007; 28: 2965-7.
- [23] Lee H, Choi W I, Nguyen M C, Cha M-H, Moon E, Ihm J. Ab initio study of dihydrogen binding in metal-decorated polyacetylene for hydrogen storage. *Phys Rev B* 2007 76 195110-1-7.
- [24] Li S, Jena P. Li- and B-decorated cis-polyacetylene: A computational study. *Phys Rev B* 2008; 77: 193101-1-4.
- [25] Yuan SW, Kirklin S, Dorney B, Liu DJ, Yu LP. Nanoporous polymers containing stereocontorted cores for hydrogen storage. *Macromolecules* 2009; 42 1554-9.
- [26] Lee H, Choi W I, Ihm J. Combinatorial search for optimal hydrogen-storage nanomaterials based on polymers. *Phys Rev Lett* 2006; 97: 056104-1-4.
- [27] Li S, Jena P. Comment on "Combinatorial search for optimal hydrogen-storage nanomaterials based on polymers". *Phys Rev Lett* 2006; 97: 209601-1-4.
- [28] Phillips AB, Shivaram BS. High capacity hydrogen absorption in transition metal-ethylene complexes observed via nanogravimetry. *Phys Rev Lett* 2008; 100: 105505-1-4.
- [29] Sun Q, Wang Q, Jena P, Kawazoe Y. Clustering of Ti on a C₆₀ surface and its effect on hydrogen storage. *J Am Chem Soc* 2005; 127: 14582-3.
- [30] Sun Q, Jena P, Wang Q, Marquez M. First-principles study of hydrogen storage on Li₁₂C₆₀. *J Am Chem Soc* 2006; 128: 9741-5.
- [31] Shevlin SA, Guo ZX. High-capacity room-temperature hydrogen storage in carbon nanotubes via defect-modulated titanium doping. *J Phys Chem C* 2008; 112: 17456-64.

- [32] Zhang CG, Zhang RW, Wang ZX, Zhou Z, Zhang SB, Chen Z. Ti-Substituted boranes as hydrogen storage materials: A computational quest for ideal combination of stable electronic structure and optimal hydrogen uptake. *Chem Eur J* 2009; 15: 5910-9.
- [33] Ivanovskaya VV, Enjashina AN, Sofronova AA, Makurina YN, Medvedeva NI, Ivanovskii AL. Quantum chemical simulation of the electronic structure and chemical bonding in (6,6), (11,11) and (20,0)-like metal-boron nanotubes. *J. Mol. Struct. (Theochem)* 2003; 625: 9-16.
- [34] Meng S, Kaxiras E, Zhang Z. Metal-diboride nanotubes as high-capacity hydrogen storage media. *Nano Lett* 2007; 7: 663-7.
- [35] Klontzas E, Mavrandonakis A, Tylianakis E, Froudakis GE. Improving hydrogen storage capacity of MOF by functionalization of the organic linker with lithium atoms. *Nano Lett* 2008; 8: 1572-6.
- [36] Cabria I, López MJ, Alonso JA. Density functional calculations of hydrogen adsorption on boron nanotubes and boron sheets. *Nanotechnology* 2006; 17: 778-85.
- [37] Zhao YF, Lusk MT, Dillon AC, Heben MJ, Zhang SB. Boron-based organometallic nanostructures: Hydrogen storage properties and structure stability. *Nano Lett* 2008; 8: 157-61.
- [38] Li YC, Zhou G, Li J, Gu B-L, Duan WH. Alkali-metal-doped B₈₀ as high-capacity hydrogen storage media. *J Phys Chem C* 2008; 112: 19268-71.
- [39] Li M, Li YF, Zhou Z, Shen PW, Chen ZF. Ca-coated boron fullerenes and nanotubes as superior hydrogen storage materials. *Nano Lett* 2009; 9: 1944-8.
- [40] Wu GF, Wang JL, Zhang XY, Zhu LY. Hydrogen storage on metal-coated B₈₀ buckyballs with density functional theory. *J Phys Chem C* 2009; 113: 7052-7.
- [41] Boustani I. Systematic ab initio investigation of bare boron clusters: m Determination of the geometry and electronic structures of B_n (n=2–14). *Phys Rev B* 1997; 55: 16426-38.
- [42] Niu J, Rao BK, Jena P. Atomic and electronic structures of neutral and charged boron and boron-rich clusters. *J Chem Phys* 1997; 107: 132-40.
- [43] Aihara J-I, Kanno H, Ishida T. Aromaticity of planar boron clusters confirmed. *J Am Chem Soc* 2005; 127: 13324-30.
- [44] Zubarev DY, Boldyrev AI. Comprehensive analysis of chemical bonding in boron clusters. *J Comput Chem* 2006; 28: 251-68.
- [45] Alexandrova AN, Boldyrev AI, Zhai H-J, Wang L-S. All-boron aromatic clusters as potential new inorganic ligands and building blocks in chemistry. *Coord Chem Rev* 2006; 250: 2811-66.
- [46] Zhai H-J, Wang L-S, Alexandrova AN, Boldyrev AI, Zakrzewski VG. Photoelectron spectroscopy and ab initio study of B₃⁻ and B₄⁻ anions and their neutrals. *J Phys Chem A* 2003; 107: 9319-28.
- [47] Zhai H-J, Wang L-S, Alexandrova AN, Boldyrev AI. Electronic structure and chemical bonding of B₅⁻ and B₅ by photoelectron spectroscopy and ab initio calculations. *J Chem Phys* 2002; 117: 7917-24.
- [48] Alexandrova AN, Boldyrev AI, Zhai H-J, Wang L-S, Steiner E, Fowler PW. Structure and bonding in B₆⁻ and B₆: Planarity and antiaromaticity. *J Phys Chem A* 2003; 107: 1359-69.
- [49] Pancharatna PD, Mendez-Rojas MA, Merino G, Vela A, Hoffmann R. Aromaticity of planar boron clusters confirmed. *J Am Chem Soc* 2004; 126: 15309-15.
- [50] Pickard CJ, Needs RJ. Ab initio random structure searching, *Psi-k Newsletter* 2010; 100: p.42.
- [51] Hyde BG, Andersson S. *Inorganic Crystal Structures*. New York John Wiley & Sons; 1989, 217-35.
- [52] Sidgwick NV, Powell HM. Bakerian Lecture: Stereochemical types and valency groups. *Proc. Roy. Soc. Lond. A* 1940; 176: 153-80.
- [53] Bjurström T. X-Ray analysis of the Fe-B, Co-B, and Ni-B systems. *Arkiv Kemi Mineral Geol* 1933; 11A: 1-12.
- [54] Mohn P, Pettifor DG. The calculated electronic and structural properties of the transition-metal monoborides. *J Phys C: Sol St Phys* 1988; 21: 2829-39.

- [55] Mohn P The calculated electronic and magnetic properties of the tetragonal transition-metal semi-borides. *J Phys C: Sol St Phys* 1988; 21: 2841-51.
- [56] Meetsma A, De Boer JL, Van Smaalen S. Refinement of the crystal structure of tetragonal Al_2Cu . *J Sol St Chem* 1989; 83: 370-2.
- [57] Mouffok B, Feraoun H, Aourag H. Electronic structure of some mono-, semi-titanium boride and diboride. *Materials Letters* 2006; 60: 1433-6.
- [58] Giannozzi P et al. Quantum espresso: a modular and open-source software project for quantum simulations of materials. *J Phys: Cond. Mat* 2009; 21: 395502-1-19.
- [59] Perdew JP, Burke K, Ernzerhof M. Generalized gradient approximation made simple. *Phys Rev Lett* 1996; 77: 3865-8.
- [60] Vanderbilt D. Soft self-consistent pseudopotentials in a generalized eigenvalue formalism. *Phys Rev B* 1990; 41: 7892-5.
- [61] Marzari N, Vanderbilt D, De Vita A, Payne MC. Thermal contraction and disordering of the Al(110) surface. *Phys Rev Lett* 1999; 82: 3296-9.
- [62] Monkhorst HJ, Pack JD. Special points for Brillouin-zone integrations. *Phys Rev B* 1976; 13: 5188-92.
- [63] Balakrishnan A, Smith V, Stoicheff BP. Dissociation energy of the hydrogen molecule. *Phys Rev Lett* 1992; 68: 2149-52.
- [64] Alapati SV, Johnson JK, Sholl DS. Using first principles calculations to identify new destabilized metal hydride reactions for reversible hydrogen storage. *Phys Chem Chem Phys* 2007; **9**: 1438-52.
- [65] Zhang Y, Morin F, Huot J. The effect of Ti-based additions on the kinetics and reactions in LiH/MgB₂ hydrogen storage system. *Int J Hydrogen Energy* 2011; 36: 5425-30.
- [66] Kurko S, Matović L, Novaković N, Matović B, Jovanović Z, Paskaš Mamula B, Grbović Novaković J. Changes of hydrogen storage properties of MgH₂ induced by boron ion irradiation. *Int J Hydrogen Energy* 2011; 36: 1184-9.
- [67] Liu BH, Zhang BJ, Jiang Y. Hydrogen storage performance of LiBH₄+MgH₂ composites improved by Ce-based additives. *Int J Hydrogen Energy* 2011; 36: 5418-24.
- [68] Vajeeston P, Ravindran P, Kjekshus A, Hjellvåg H. Crystal structure of KAlH₄ from first principle calculations. *J Alloys Comp* 2004; 363: L1-11.
- [69] Li F, Zhao J, Chen Z. Hydrogen storage behaviour of one-dimensional TiB_x chains. *Nanotechnology* 2010; 21: 134006-1-6.